

- <sup>1</sup>R. A. Soref and H. W. Moos, *J. Appl. Phys.* **35**, 2152 (1964).  
<sup>2</sup>R. K. Chang, J. Ducuing, and N. Bloembergen, *Phys. Rev. Letters* **15**, 415 (1965).  
<sup>3</sup>F. C. Parsons and R. K. Chang, *Opt. Commun.* **3**, 173 (1971).  
<sup>4</sup>J. J. Wynne, *Phys. Rev. Letters* **27**, 17 (1971).  
<sup>5</sup>E. Yablonovitch, N. Bloembergen, and J. J. Wynne, *Phys. Rev. B* **3**, 2060 (1971).  
<sup>6</sup>R. E. Slusher, C. K. N. Patel, and P. A. Fleury, *Phys. Rev. Letters* **18**, 77 (1967); C. K. N. Patel and R. E. Slusher, *Phys. Rev.* **167**, 413 (1968).  
<sup>7</sup>P. A. Wolff and G. A. Pearson, *Phys. Rev. Letters* **17**, 1015 (1966).  
<sup>8</sup>C. K. N. Patel, R. E. Slusher, and P. A. Fleury, *Phys. Rev. Letters* **17**, 1011 (1966).  
<sup>9</sup>B. Lax, W. Zawadzki, and M. H. Weiler, *Phys. Rev. Letters* **18**, 462 (1967).  
<sup>10</sup>E. O. Kane, *J. Phys. Chem. Solids* **1**, 249 (1957).  
<sup>11</sup>P. N. Butcher and T. P. McLean, *Proc. Phys. Soc. (London)* **81**, 219 (1963).  
<sup>12</sup>P. A. Wolff, *Phys. Rev. Letters* **16**, 225 (1966).  
<sup>13</sup>C. R. Pidgeon and R. N. Brown, *Phys. Rev.* **146**, 575 (1966).  
<sup>14</sup>N. Van Tran and C. K. N. Patel, *Phys. Rev. Letters* **22**, 463 (1969).

## Optical Properties of Substitutional Donors in ZnSe

J. L. Merz, H. Kukimoto, K. Nassau, and J. W. Shiever  
*Bell Telephone Laboratories, Murray Hill, New Jersey 07974*

(Received 22 March 1972)

Five substitutional donors have been observed in ZnSe: Al, Ga, In, Cl, and F. By measuring the  $I_2$  lines and the two-electron transitions associated with each, the donor binding energies have been determined. These are found to be close to the effective-mass value and vary from 26.3 meV for Al to 29.3 meV for F. Excited states of the complex formed by the exciton bound to the neutral donor were observed both in the region above the  $I_2$  lines and in the two-electron transitions. The electron effective mass was measured from the Zeeman splitting of the  $2p$  states of the donors to be  $m = (0.16 \pm 0.01)m_e$ . For each donor, a doublet was also observed at lower energy than the  $I_2$  lines; these doublets are believed to be the corresponding  $I_3$  lines. The binding energies of excitons both to the ionized and the neutral donors were found to vary linearly with the donor central-cell correction. Most of these results are closely analogous to the properties of CdS and CdSe.

### I. INTRODUCTION

Considerable progress has been made recently toward understanding the nature of donors and acceptors in the II-VI compounds CdS and CdSe by studying the optical properties of large numbers of these crystals which have been systematically doped with the appropriate impurities. Through a detailed study of the Cl donor in CdS, Henry and Nassau<sup>1</sup> unraveled the complicated two-electron transitions and identified excited states of the exciton bound to the neutral donor, the so-called  $I_2$  line. This was extended by Nassau *et al.*,<sup>2</sup> who determined the chemical identity and binding energies of six substitutional donors in CdS. The same authors have recently studied the optical properties of shallow acceptors in CdS and CdSe,<sup>3</sup> and have identified the two-electron transitions of a donor in CdSe.<sup>4</sup> Comparatively little is known about the substitutional impurities in the Zn compounds, however. In particular, the properties of ZnSe, a wide band gap ( $\sim 2.8$  eV),  $n$ -type semiconductor which exists in either the cubic or hexagonal form, are little understood.

In this paper, the properties of the substitutional

donors in cubic ZnSe are investigated in detail. The  $I_2$  lines resulting from the radiative recombination of excitons bound to neutral donors have been chemically identified for five different donors, along with the corresponding  $I_3$  lines (excitons bound to the ionized donors). Two-electron transitions are also identified for four of the donors. These transitions also result from the radiative recombination of an exciton bound to a neutral donor, but instead of leaving the donor in its ground  $1s$  state (which gives the  $I_2$  line), the donor electron is left in an excited state ( $2s$ ,  $2p$ , etc.). Two-electron transitions were first identified in GaP,<sup>5</sup> and shortly thereafter were observed by Reynolds *et al.* in the II-VI compounds CdS,<sup>6</sup> CdSe,<sup>7</sup> and ZnO.<sup>8</sup> In addition to these two-electron transitions in ZnSe, it is also found that a number of two-electron transitions arise from excited states of the three-particle bound exciton complex, that is, the two electrons and one hole that are bound to the ionized donor impurity. Such excited states have also been seen by Henry *et al.*,<sup>1,4</sup> and by Malm and Haering<sup>9</sup> using luminescence excitation experiments in CdS. A fifth donor (F) has been identified by the observation of its  $I_3$  lines.

The behavior of the donors in ZnSe reported in this paper is found to be strongly analogous to the properties of CdS<sup>1,2</sup> and CdSe.<sup>4</sup> From the identification of the two-electron transitions, the electron effective mass has been determined to be  $m = (0.16 \pm 0.01)m_e$ , where  $m_e$  is the free-electron mass. The binding energies for each of the donors have been accurately measured, and all are found to be quite close to the effective-mass binding energy of 28.8 meV. The diamagnetic shift of the donor 2s state has also been observed experimentally and found to agree with the shift predicted on the basis of the above parameters.

This work is the second of a series of three papers on ZnSe originating from this laboratory. In the first (hereafter referred to as DM), Dean and Merz<sup>10</sup> reported the first observation of discrete donor-acceptor pair lines in any II-VI compound. These lines result from the recombination of an electron bound to a donor with a hole bound to an acceptor; a series of discrete lines are observed because of the difference in the Coulomb interaction between these centers for their various spatial separations allowed by the lattice. Additional pair spectra have subsequently been observed which are associated with the same donors identified in the present paper. These pair spectra are presented in the third paper of this series<sup>11</sup> (referred to as MNS), along with a discussion of the dominant acceptors in ZnSe which are believed to participate in these pair spectra.

## II EXPERIMENTAL TECHNIQUES

### A. Crystal Preparation

Crystals were grown from the vapor phase in a flowing stream of forming gas (85% N<sub>2</sub>, 15% H<sub>2</sub>). Impurity contamination was minimized by the use of an all-quartz apparatus and rapid growth (3–4 h) in a high gas flow (10 cm/sec at the growth temperature), as described previously.<sup>12</sup> In certain cases, a high-purity alumina ceramic inner tube was used.

The sublimation temperature was 1250 °C and crystals grew in a temperature gradient of 15 °C/cm near 1050 °C. The starting material was Eagle-Picher, ultra-high-purity grade containing about 5 ppm Ca, Fe, Cu, Mg, Al, and Si; about 1 ppm Pb and Ag; and less than 1 ppm Ga, In, and F. Growth in the absence of added impurities increased the Si content to about 50 ppm, but left the other concentrations unchanged. Best results were obtained when excess Zn was added to the charge.

Chlorine was added by passing part of the gas stream through concentrated HCl and then through concentrated H<sub>2</sub>SO<sub>4</sub>. Aluminum, indium, and gallium were added by mixing the metal with the feed

ZnSe. Attempts to introduce Br and I as described previously<sup>12</sup> were unsuccessful. F was added by diffusion with ZnF<sub>2</sub> at 600 °C in a sealed quartz ampoule.

### B. Photoluminescence Measurements

Photoluminescence was excited by a Coherent Radiation Laboratory argon ion laser operating in the ultraviolet at  $\sim 3500 \text{ \AA}$ .<sup>13</sup> Up to 100 mW could be obtained from this laser, although it was usually found that a power of 20–30 mW was sufficient to excite intense luminescence without heating the samples above the bath temperature. The crystals were mounted in a strain-free fashion and immersed in liquid helium which could be pumped below the  $\lambda$  point. For studying thermalization effects, liquid hydrogen could also be used. The luminescence was focused onto the entrance slit of a Jarrell Ash 2-m Czerney-Turner spectrometer, with an 1180-groove/mm grating blazed at 7500 Å which had a dispersion of  $\sim 0.8 \text{ \AA/mm}$  in third order. The spectra could be detected either photographically (for accurate measurements of energy separations and Zeeman splittings of spectral lines) or photoelectrically (for intensity measurements) with an EMI model No. 9558 photomultiplier thermoelectrically cooled to  $-25 \text{ }^\circ\text{C}$ . The glass helium cryostat was suspended between the poles of a Varian electromagnet capable of producing a field of 32 kG at the position of the sample.

## III. RESULTS AND DISCUSSION

### A. Observed Spectra

The low-temperature luminescence spectra observed from good quality nominally undoped crystals were usually quite complicated; a typical example is shown in Fig. 1. The strongest lines in the spectra are usually the  $I_2$  lines resulting from excitons bound to the neutral donors which are inadvertently present in these crystals at low concentrations. These  $I_2$  lines are observed at approximately 2.797 eV; above them, and tending toward the broad peak of the free exciton at  $\sim 2.802 \text{ eV}$ , is a series of sharp lines which have been identified as excited states of the bound exciton complex, as will be discussed later. Below the  $I_2$  lines, between 2.794 and 2.797 eV, are often seen one or more doublets, with a strong lower-energy line and a weaker higher-energy component. There is strong evidence that these doublets result from the recombination of excitons bound to the ionized donors; i. e., these are the so-called  $I_3$  lines.

Below all of these donor-associated spectral features lie two strong lines referred to as  $I_1^X$  and  $I_1^{\text{DEEP}}$  in Fig. 1, because of the accumulation of evidence that they result from the recombination

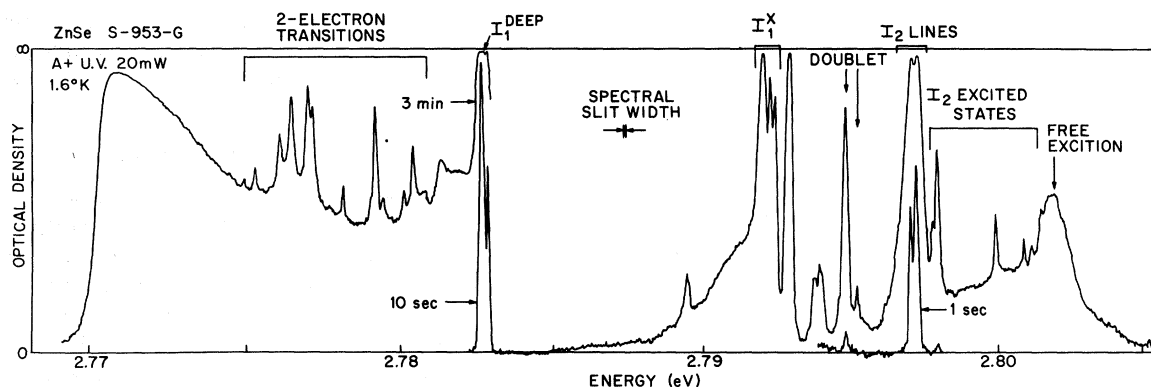


FIG. 1. Photoluminescence vs photon energy of a nominally undoped sample of ZnSe showing the various spectral features discussed in the text. This spectrum is a densitometer trace of a photographic plate; exposure times are indicated.

of excitons bound to neutral acceptors (so-called  $I_1$  lines). Both of these lines exhibit the strong series of LO phonon replicas which are characteristic of the  $I_1$  lines in CdS and CdSe,<sup>3</sup> and it was pointed out by DM that the  $I_1^{\text{DEEP}}$  line (referred to simply as the  $I_1$  line in that work) exhibited typical  $I_1$  behavior when crystals were heat treated in Zn vapor or in vacuum. For example, this line was reduced in intensity when heated in Zn vapor at 700 °C, although the intensity changes were much less dramatic than those observed for CdS annealed in Cd vapor. On the other hand, the  $I_1^{\text{X}}$  line (called  $I_x$  by DM), which in high resolution is found to be a triplet, is significantly increased by heat treatment in Zn, and was believed to be associated with the pair spectrum reported by DM because this heat treatment also made the pair lines visible. There is more recent evidence that the line  $I_1^{\text{X}}$  results from the substitutional Li acceptor at a Zn site, although this has yet to be conclusively proven. The origin of both of these  $I_1$  lines will be discussed in detail in the context of the donor-acceptor pair spectra presented by MNS, and will therefore not be considered further below.

Finally, in the low-energy region of Fig. 1, the weak two-electron transitions are superimposed on the broad background tail below the  $I_1^{\text{DEEP}}$  line. This background, with its sharp cutoff at approximately 2.77 eV, is believed to be an acoustic-phonon replica of the line  $I_1^{\text{DEEP}}$ , although the LO-phonon replica of the free exciton may contribute to its intensity. The visibility of the two-electron transitions is best for crystals with a weak  $I_1^{\text{DEEP}}$  line.

The complexity of the spectrum shown in Fig. 1 for an undoped crystal illustrates the difficulty in identifying the various spectral lines. In fact, the assignments of  $I_2$  lines, their excited states and associated two-electron transitions, were possible only after comparing the spectra obtained from a

large number of doped and nominally undoped crystals. This sort of comparison is illustrated in Fig. 2, where spectra are shown in greater detail for two undoped crystals and one doped with Cl. For simplicity, only the two spectral regions of interest for the study of the donors are shown. In this figure, the double-headed arrows indicate the principal  $I_2$  line obtained in each case; additional arrows show the corresponding  $I_2$  excited states, doublets, and two-electron transitions. Note that for a small shift in energy between two different  $I_2$  lines (corresponding to two different donors), an even smaller energy shift is observed for the excited states, whereas a large energy shift occurs for the doublets. (In each case, the arrow points to the strong lower-energy component of the doublet.) For the two-electron spectra, five arrows indicate the principal transitions associated with each donor, although some of these lines appear in other spectra because more than one donor is present in each crystal. [For the spectrum in Fig. 2(a) only four arrows are shown for the two-electron transitions, since two of the transitions overlap.]

The similarities between the two-electron spectra for different crystals become more obvious if the spectra are shifted in energy relative to each other. This is done in Fig. 3 for the same three crystals shown in Fig. 2. The energy axis has been uniformly shifted by an amount and direction indicated by the calibration lines. Six different transitions are clearly indicated by the solid lines for each donor; the broken lines show the transitions which belong to other donors.

By comparing a large number of spectra from different crystals in the manner illustrated by Figs. 2 and 3, each feature of the spectrum has been identified, and an energy-level diagram for the exciton effects has been proposed. This is shown in Fig. 4. At the bottom is shown an

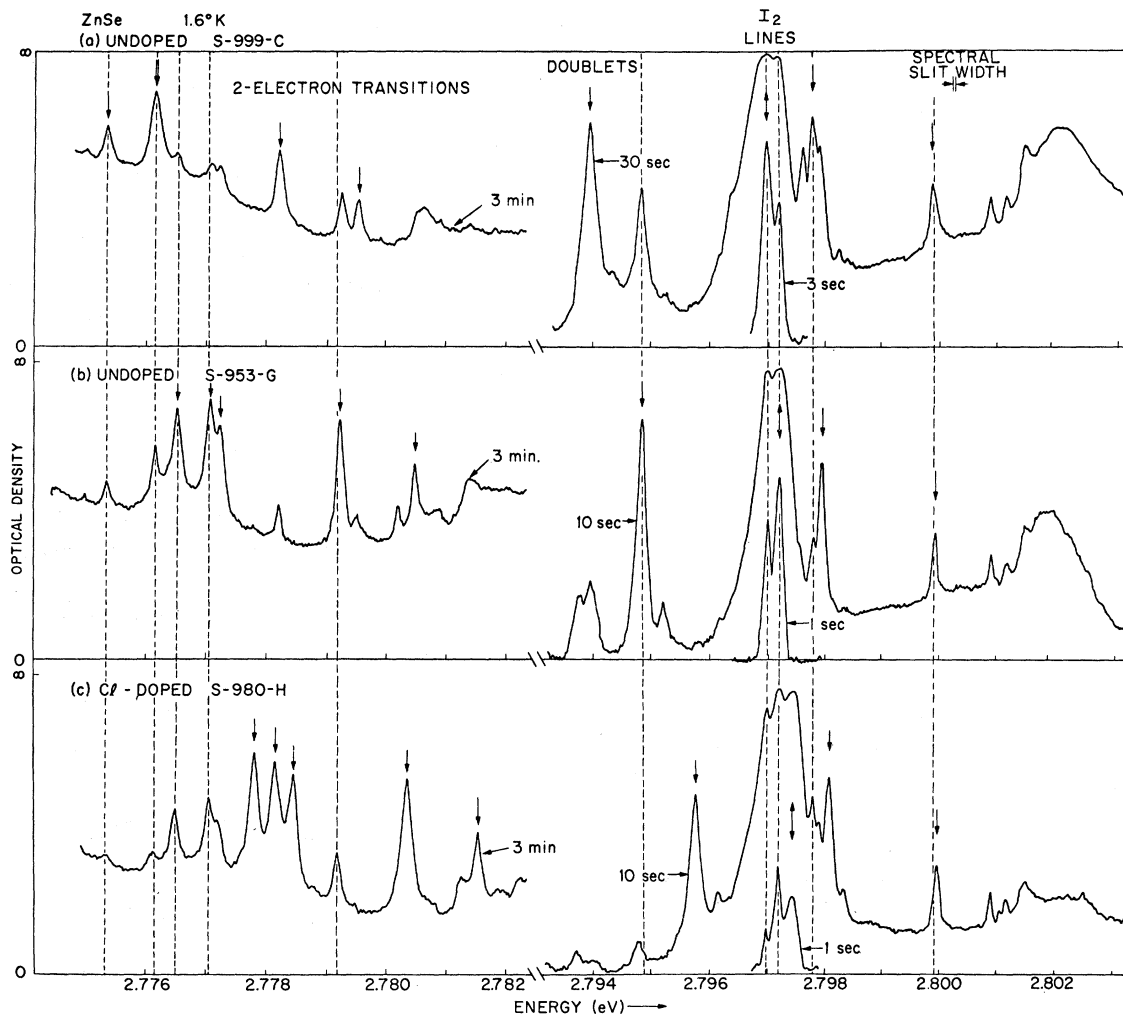


FIG. 2. Photoluminescence of two nominally undoped samples of ZnSe and one doped with Cl. Only the two-electron transitions and the region near the  $I_2$  lines are shown. The double-headed arrows indicate the principal  $I_2$  line for each crystal; other arrows indicate the other spectral features which accompany the principal  $I_2$  line. By comparing spectra such as this, lines resulting from extraneous donors have been eliminated, and the features resulting from the single donor have been determined.

idealized spectrum for a single donor; that is, all extraneous lines resulting from other donors have been removed. Above it, the energy-level diagram shows the ground and excited states for the exciton bound to the neutral donor (three-particle system), and the ground state ( $1s$ ), and excited states ( $2s$  and  $2p$ ) for the neutral donor alone. The principal transition is the  $I_2$  line, which is now labeled  $I_{20}$  for clarity; the transition originates from the ground state of the bound exciton ( $I_{20}$  state) and terminates with the donor in its ground state. The weak sharp spectral lines at higher energy originate from excited states of the bound exciton complex (labeled  $I_{2\alpha}$ ,  $\alpha = a, b, c, d$ ) and also terminate on the donor ground state. The nature of each of the two-electron transitions observed is now clear from this diagram; these transitions also originate

from the ground and excited exciton states, but leave the donor in an excited  $2s$  or  $2p$  state. The labeling of these transitions indicates whether the donor is left in an excited  $s$  or  $p$  state, while the subscript indicates the initial state of the exciton.

TABLE I. Energies of bound excitons and two-electron transitions (eV).

Spectral line	Donor					
	Al	Cl	Ga	In	F	
$I_{20}$	2.79754	2.79745	2.79718	2.79697	2.7969 <sup>a</sup>	
$I_3$	Weak	2.79653	2.79614	2.79518	2.79429	2.79388
	Strong	2.79615	2.79574	2.79477	2.79388	2.79348
$2-e$	$s_0$	2.77867	2.77812	2.77700	2.77606	...
	$p_0$	2.77840	2.77779	2.77646	2.77528	...

<sup>a</sup>Extrapolated from data plotted in Fig. 7.

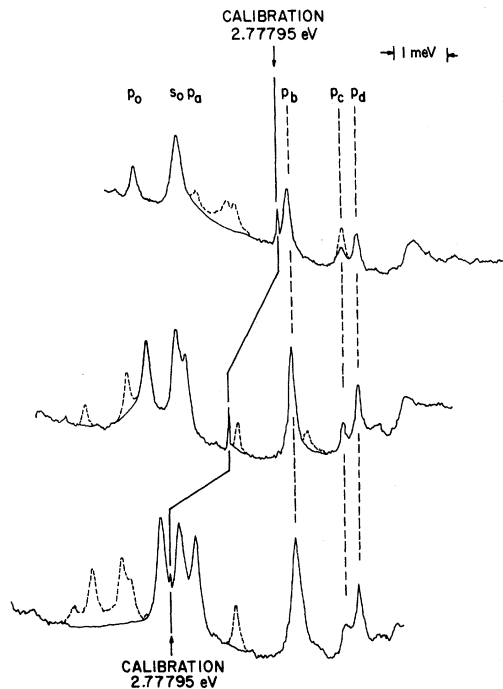


FIG. 3. Two-electron transitions of the same three crystals shown in Fig. 2, but with the energy axis shifted by amounts indicated by the solid line joining the 2.77795-eV calibration line in each spectrum. Broken lines are due to extraneous donors (overlap from other two-electron transitions). The notation for the  $s$  and  $p$  states shown is defined in Fig. 4. The solid lines illustrate the evident similarities in the two-electron spectra for different donors. Chemical-doping experiments described in the text have proved that these spectra belong to the donors In, Ga, and Cl (from top to bottom).

The energies of all the spectral lines have been measured to  $\pm 0.02$  meV for four different donors. These energies are listed in Table I for the fundamental lines  $I_{20}$ ,  $p_0$ ,  $s_0$ , and the two components of the doublets (believed to be  $I_3$  lines). The chemical identification of the donors will be discussed below in Sec. III B; the assignment of the orbital  $s$  and  $p$  states of the donor has been made by observing their behavior in a magnetic field, as shown in Sec. III C. Note that the energy separation of the lines  $I_{20}$  and  $p_0$  experimentally determines the energy separation between the donor  $2p$  and  $1s$  states, which is a measure of the central-cell correction. This is a significant quantity, necessary for determining the donor binding energy, and will be discussed further below.

One important test for the proposed energy-level diagram of Fig. 4 is to measure the energy differences  $\Delta_\alpha$  in two ways: from the separation of the bound exciton lines  $I_{2\alpha}$  and from the two-electron transitions, as shown in the figure. Both of these measurements should give the energy of the exciton

excited state above its ground state. The energy differences  $\Delta_\alpha$  measured both ways are compared in Table II. In every case these differences agree to well within experimental accuracy.

### B. Chemical Identification of the Donors

For most of the donors discussed in this paper, the sharpest spectral lines have been observed in nominally undoped crystals, resulting from inadvertent contamination either in the starting powder or during the growth of the crystals. The process of sorting out the spectral features proper to an individual donor, as yet unidentified, was achieved

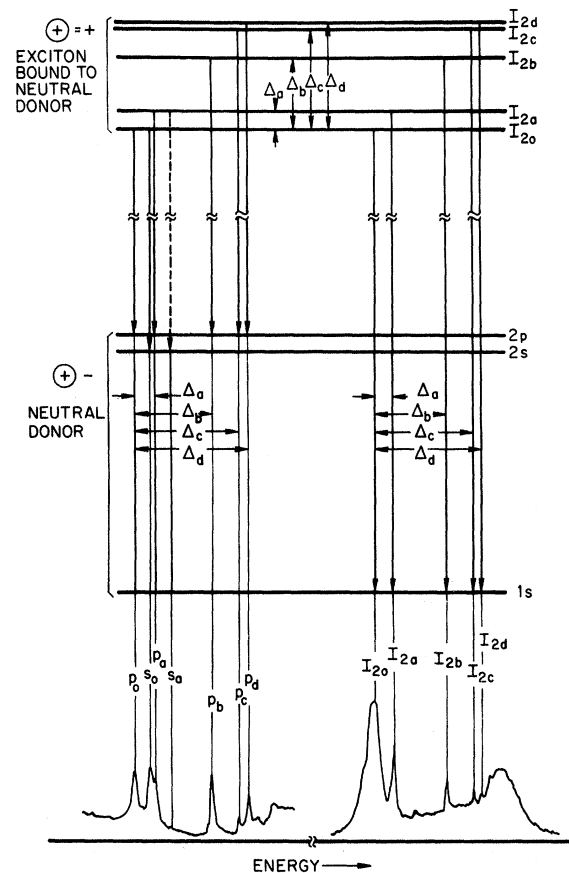


FIG. 4. Idealized spectrum (at bottom) of the two-electron transitions and  $I_2$  lines, and the energy-level diagram showing how these transitions arise. The ground and excited states of the three-particle complex composed of an exciton bound to a neutral donor are indicated by the levels  $I_{20}$  and  $I_{2\alpha}$ ,  $\alpha = a, b, c,$  and  $d$ . Transitions from these states may leave the neutral donor in its ground  $1s$  state ( $I_2$  lines themselves) or in an excited  $2s$  or  $2p$  state (two-electron transitions). Note that the energy spacings  $\Delta_\alpha$  of the bound-exciton states are reflected both in the  $I_2$  lines and in the two-electron transitions. The idealized spectrum is taken from Fig. 2(b), but with extraneous lines (belonging to other donors) omitted.

TABLE II. Energy differences between bound-exciton lines and two-electron transitions (meV).

		Donor			
		Al	Cl	Ga	In
$\Delta_a$	$I_{2a}-I_{20}$	0.62	0.65	0.72	0.82
	$p_a-p_0$	0.61	0.64	0.71	0.79
$\Delta_b$	$I_{2b}-I_{20}$	2.45	2.53	2.74	2.86
	$p_b-p_0$	2.44	2.52	2.71	2.86
$\Delta_c$	$I_{2c}-I_{20}$	3.36	3.45	3.73	3.88
	$p_c-p_0$	3.32	3.46	3.70	3.87
$\Delta_d$	$I_{2d}-I_{20}$	3.64	3.74	4.01	4.16
	$p_d-p_0$	3.61	3.73	3.98	4.15

by comparing spectra from many different runs, as described above, and these spectra were generally used for energy measurements because of the sharp lines observed. However, the actual chemical identification of the donors was carried out by doping the crystals during growth. Usually it was found that the actual doping run (the growth run in which the impurity of interest was added) was heavily overdoped, giving very broad spectral features with no resolvable lines. Subsequent runs were then made without adding more of the impurity, using the contamination of the furnace tube to produce a strong  $I_2$  line. This  $I_2$  line would become progressively weaker and sharper as the amount of contamination decreased with each successive run. This procedure is described in more detail by Nassau and Shiever.<sup>12</sup>

In this way, the group-III donors Al, Ga, and In have been identified. Two of the group-VII donors have also been identified, Cl by doping during growth and F by diffusion. The evidence for some of these impurities is stronger than for others, however. In particular, it is felt that the evidence for Cl and Ga is convincing, the case for In is only slightly weaker, while the evidence for Al and F is somewhat questionable. There is no evidence for the presence of the simple substitutional donors due to Br and I, although doping with these impurities was attempted. Each of these impurities will be discussed below, starting with those for which the chemical evidence is the most convincing.

(a) *Chlorine*. The presence of Cl in the growth tube was a necessary and sufficient condition for the observation of the line labeled  $I_{20}^{Cl}$  and its associated spectrum (excited states,  $I_3$  doublet, etc.). In two runs the  $I_{20}^{Cl}$  line was very strong but broad; when the flow of gas through the HCl source was cut in half,  $I_{20}^{Cl}$  was sharp and dominant, and the corresponding two-electron transitions were clearly seen. A subsequent run relying on Cl contamination from the earlier runs (flow through HCl eliminated) did not show  $I_{20}^{Cl}$ , but instead a higher-

energy  $I_2$  line, believed to be  $I_{20}^{Al}$ , was seen. This trend in Cl concentration is also observed in these same crystals by activation analysis, although the range of Cl concentration observed is quite small. The results of chemical analyses are shown in Table III.

(b) *Gallium*. The results of a Ga-doping experiment are shown in Fig. 5(a) where the second, third, fourth, and sixth runs are shown for a set of Ga doping runs; Ga was added only to the first run. In the second and third runs, the  $I_{20}^{Ga}$  line is still too broad for positive identification, in the fourth run, it has sharpened considerably, and by the sixth run another donor (Al) becomes visible. This large variation in Ga concentration is also evident by chemical analysis, as shown in Table III. Even in nominally undoped samples (fresh uncontaminated furnace tube)  $I_{20}^{Ga}$  is usually observed, and Ga appears to be one of the two most common contaminants in ZnSe (along with In). This probably results from the fact that Ga and In are common low-level impurities in Zn.

(c) *Indium*. The results for In are very similar to those for Ga, with the exception that the maximum attainable concentrations of this impurity are much lower. This is seen both in the resulting spectra [Fig. 5(b)] and in the chemical analysis (Table III).

(d) *Aluminum*. The line referred to in Fig. 5 as  $I_{20}^{Al}$  is one that appears very frequently in these crystals, especially when doping experiments are attempted, but is never very strong. The strength of this line usually increases with successive "contamination" runs as can be seen in Fig. 5: The strength of  $I_{20}^{Al}$  grows relative to  $I_{20}^{Ga}$  and  $I_{20}^{In}$  for successive runs. This effect has also been pointed out for Cl doping, and has been observed in unsuccessful attempts to dope ZnSe with the other halogens. It appears, therefore, that as successive runs begin to attack the quartz growth tubes, the donor responsible for this line becomes more prevalent. A similar effect has also been noticed in "seed"

TABLE III. Impurity concentrations in vapor-grown ZnSe crystals (ppm).

Impurity <sup>a</sup>	Pure crystals	"Good" crystals <sup>b</sup>	Highest observed
Al	~5	~5	~5
Cl	0.3	0.5	1.0
Ga	<1	~50	>10 000
In	0.1	0.2	500

<sup>a</sup>Analyses by emission spectroscopy except Cl, which was done by activation analysis by Kim. All crystals were heavily etched in acid to remove any possible surface contamination.

<sup>b</sup>Crystals showing sharp dominant spectral features.

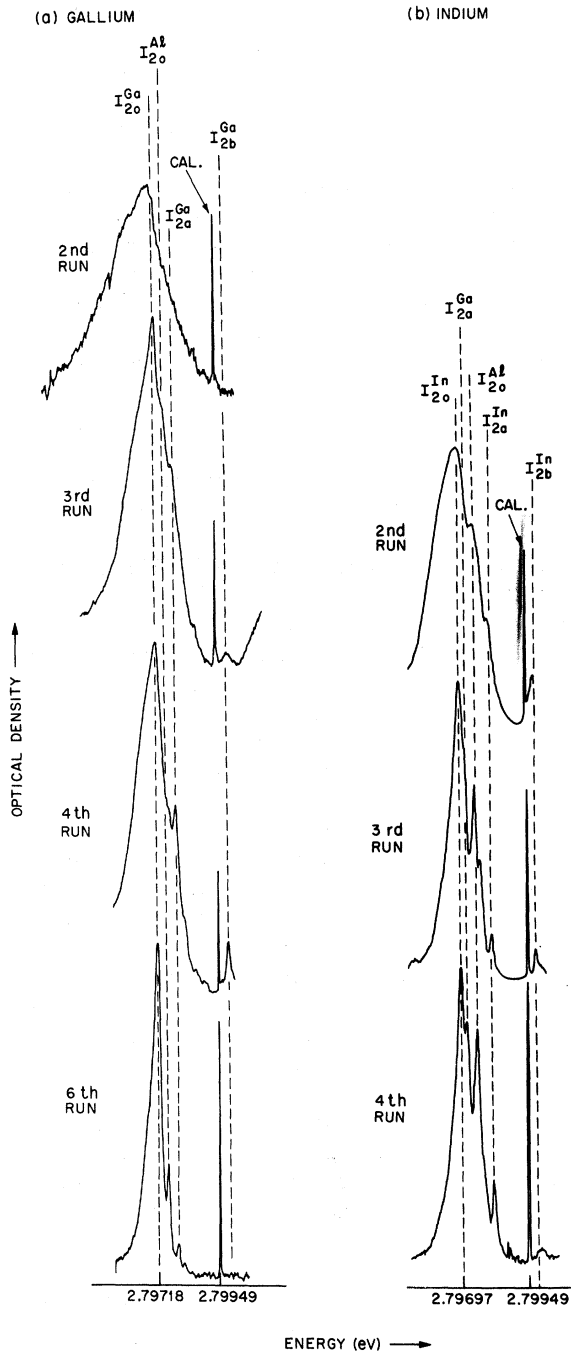


FIG. 5. Densitometer traces of the  $I_2$  lines for crystals doped with different concentrations of (a) gallium and (b) indium. In each case, the impurity was added to the first run, not shown because lines were too broadened by overdoping to be resolved. In the succeeding runs (shown here) doping was achieved by the contamination of the furnace tube produced during the first run. As the contamination is reduced by successive runs, the broad dominant  $I_2$  line sharpens to become the appropriate  $I_{20}$  line, either Ga or In. Note that  $I_{20}^{Al}$  is usually present, and becomes stronger relative to other  $I_2$  lines in the later runs (cf. text).

runs: The  $I_{20}^{Al}$  line is much stronger for the first run in a new quartz tube than for the second. Aluminum, of course, is a common contaminant in quartz. Attempts to dope crystals with Al tend to corroborate the identification of the  $I_{20}^{Al}$  line, but not in dramatic fashion. The best results were obtained when Se was mixed with the Al dopant in the ZnSe, and excess Zn was also present;  $I_{20}^{Al}$  then behaved in the expected fashion for successive runs. Attempts to produce a strong line by using alumina tubing instead of quartz were unsuccessful, however; the  $I_{20}^{Al}$  line was sharp but weak.

Perhaps the best evidence that  $I_{20}^{Al}$  is indeed due to the simple Al donor will be offered by MNS, who show that pair spectra with discrete pair lines have been observed which are definitely associated with each of the three  $I_2$  lines  $I_{20}^{Al}$ ,  $I_{20}^{Ga}$ , and  $I_{20}^{In}$ . Analysis of each of these pair spectra shows that they are all type I; that is, both the donor and the acceptor are on the same sublattice. Furthermore, the binding energies obtained from the pair spectra agree with those measured in this paper from the  $I_2$  lines and the two-electron transitions. Finally, the pair spectrum corresponding to the  $I_{20}^{Al}$  line was clearly observed in crystals to which Al was added during growth. All of this evidence then strongly suggests that the  $I_{20}^{Al}$  line must result from a group-III donor at a Zn site, and it appears at an energy consistent with the Al donor in the series Al, Ga, In. Note, however, that the actual concentrations of Al attainable are very insensitive to various doping attempts; Al was never present in concentrations greater than 5 ppm (Table III).

(e) *Fluorine.* Attempts to dope ZnSe with F by diffusion were made by sealing suitable crystals in evacuated quartz ampoules with  $ZnF_2$  and heating to temperatures between 450 and 800 °C. In some crystals, heated at 600 °C, new low-energy doublets were observed, which are believed to be the  $I_3$  lines associated with the substitutional F donor. A corresponding  $I_2$  line was not observed, but this would occur at an energy unresolvable from the  $I_{20}^{In}$  line, which was also present. The identification of the  $I_3$  lines is discussed further in Sec. III D b.

(f) *Bromine and iodine.* Attempts were made to dope with Br and I by passing part of the forming gas through HBr or warmed I. No spectral features were observed in the vicinity of the bound exciton lines which could be attributed to either of these impurities. However, this doping procedure did significantly affect the crystals, since a strong broad luminescence band peaking at about 2 eV was observed at room temperature from the more heavily doped of these samples.<sup>14</sup> Similar luminescence is observed from samples heavily doped with Al, Ga, In, and Cl, and is believed to be a result from a deep donor-associated complex.

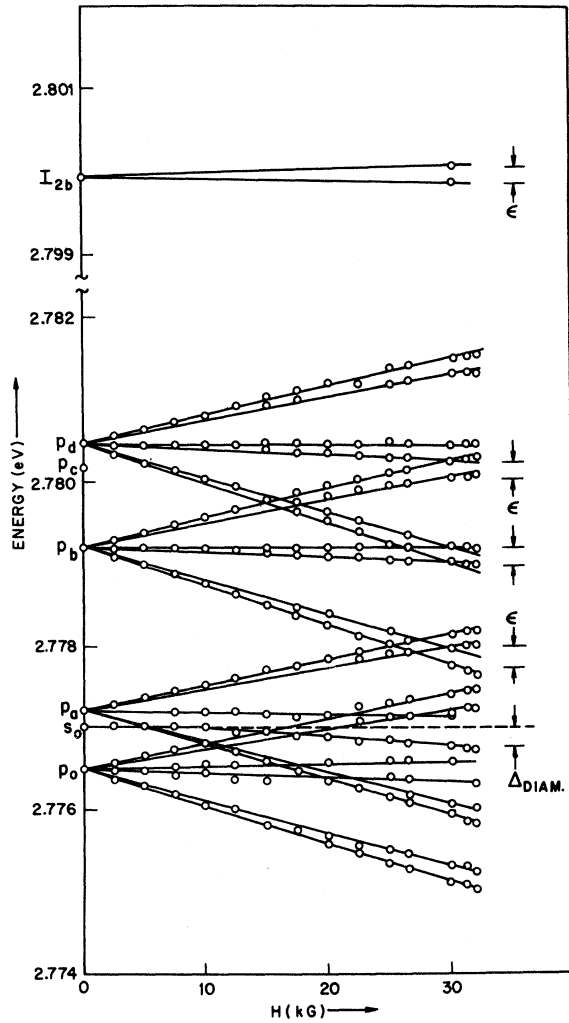


FIG. 6. Zeeman behavior of the two-electron transitions for the Ga donor as a function of magnetic field, at 1.6 °K. The  $p$  states exhibit a gross triplet splitting, with fine structure determined by the splitting of the corresponding bound-exciton state. For example, the splitting  $\epsilon$  of the three components of  $p_b$  is equal to the splitting of the exciton  $I_{2b}$  line. ( $\epsilon$  is shown for  $H=30$  kG.) The  $s_0$  state does not split but exhibits a diamagnetic shift, whose magnitude at 30 kG is indicated by  $\Delta_{\text{diam}}$ . (Crystal S-953-G shown in Fig. 1 was used for these data.)

### C. Two-Electron Transitions

The actual identification of  $s$  and  $p$  states in the two-electron spectrum has been made by their Zeeman splitting, shown in Fig. 6 for Ga. Four  $p$  states are shown, each of which splits into three lines, as expected, with fine structure determined by the splitting of the corresponding  $I_2$  line. For example, the three lines of  $p_b$  split into doublets, with spacing  $\epsilon$  equal to the splitting of  $I_{2b}$ . (In the figure,  $\epsilon$  is shown for the splittings at  $H=30$  kG.) The splittings of the state  $p_c$  are not shown, be-

cause this transition is too weak to follow as a function of  $H$  (cf. Fig. 3). Some of the other excited exciton lines  $I_{2\alpha}$  show more complicated splittings than the simple doublet of  $I_{2b}$ ; these splittings are not necessarily reproduced exactly in the fine structure of the two-electron transitions. However, the physical mechanism giving rise to the excited states  $I_{2\alpha}$  is not presently understood; it is therefore not possible to calculate selection rules and thereby account exactly for the details of the two-electron Zeeman splittings. Nevertheless, it is clear that the  $p$  states have been correctly identified, that they correspond with the states of the bound exciton complex as indicated by their subscripts, and that the fine structure reflects degeneracies within the excited exciton states themselves. From the  $g$  factor of the gross splitting of these  $2p$  states, the electron effective mass  $m$  can be measured:

$$m = 2m_e/g = (0.16 \pm 0.01)m_e.$$

This agrees with the value of  $m = 0.17m_e$  measured by Marple.<sup>15</sup> The effective-mass binding energy  $E_0$  is then given by

$$E_0 = (m/m_e \epsilon_s^2) E_h = 28.8 \pm 2.4 \text{ meV},$$

where  $E_h$  is the hydrogenic binding energy. The error is primarily determined by the sensitivity of  $E_0$  to the static dielectric constant  $\epsilon_s$ ; the low-temperature value  $\epsilon_s = 8.66$  was used above, as determined by Roberts and Marple.<sup>18</sup>

The donor  $2s$  state should not split in a magnetic field but instead exhibits a diamagnetic shift, which can be calculated from the parameters given above to be

$$\Delta_{\text{diam}} = (13/2E_0) (\mu_B H m_e / m)^2 = 0.26 \pm 0.06 \text{ meV},$$

where  $\mu_B$  is the Bohr magneton. The observed diamagnetic shift, measured from the data of Fig. 6, is in good agreement:

$$\Delta_{\text{diam}} = 0.22 \pm 0.02 \text{ meV}.$$

### D. Exciton Binding Energies

#### (a) Excitons bound to neutral donors— $I_2$ lines.

From the energies of the  $I_{20}$  lines listed in Table I, the exciton binding energies have been determined for each of the four donors identified in this study. These are plotted as a function of the central-cell parameter  $(E_{2p} - E_{1s})$  in Fig. 7, along with the binding energies for the first excited state  $I_{2a}$  of the bound exciton complex and the strong and weak components of the doublets ( $I_3$  lines). The exciton binding energies were obtained by subtracting the values of  $I_{20}$  and  $I_3$  given in Table I from the energy of the  $A$  exciton, taken to be 2.8015 eV. This value was taken from the free exciton peak in the luminescence spectrum in Fig. 1; no cor-



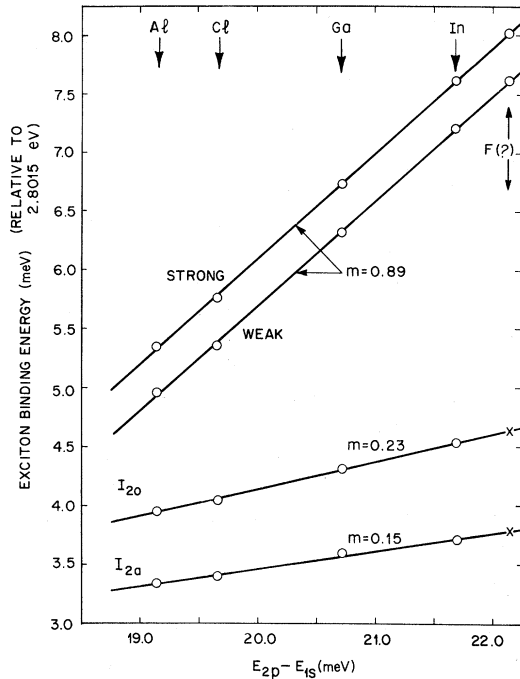


FIG. 7. Exciton binding energies as a function of the central-cell parameter  $E_{2p} - E_{1s}$  for the four donors chemically identified in this work. The free-exciton energy is taken to be 2.8015 eV. The slopes ( $m$ ) of the straight lines have been determined from a least-squares fit to the data points. The  $I_3$  doublet has been observed for F, but the corresponding  $I_2$  lines are not resolvable from In, which is always present in these crystals.

rection was made for self-absorption effects. The  $A$  exciton energy given by Segall and Marple<sup>17</sup> is 2.799 eV. The central-cell parameter ( $E_{2p} - E_{1s}$ ) is obtained by finding the difference between the  $I_{20}$  and  $p_0$  energies given in Table I.

The results shown in Fig. 7 are remarkably linear. This was also found for the donors in CdS,<sup>2</sup> and is another statement of the empirical law observed by Haynes for the donors in Si.<sup>18</sup> The lines drawn in Fig. 7 were obtained by a least-squares fit to the data points, and the slopes were calculated from this fit. The slope of the  $I_2$  line for ZnSe,  $m(I_{20}) = 0.23$ , is quite close to the result of Nassau *et al.*<sup>2</sup> for CdS:  $m(I_{20}) = 0.28$ . For the excited states of the bound exciton complex, the slope approaches zero for the more highly excited states. Thus,  $m(I_{2a}) = 0.15$ , while  $m(I_{2d}) \approx 0$ .

The variation of the exciton binding energy for different chemical donors shown in Fig. 7 is clearly a central-cell effect; in fact, Baldereschi has recently "derived" Haynes's rule by the following simple arguments.<sup>19</sup> The donor binding energy  $E_D$  can be written

$$E_D = E_0 + PV,$$

where  $E_0$  is the effective-mass binding energy,  $V$  is a square-well potential in the central cell of the donor, and  $P$  is the probability that the donor electron is in the central cell. A similar expression holds for the binding energy of the bound exciton,  $E_{BX}$ :

$$E_{BX} = E'_0 + P'V,$$

where  $E'_0$  and  $P'$  now refer to the exciton;  $P'$  is the probability of the bound exciton electrons to be in the central cell. Combining these two equations gives

$$\begin{aligned} E_{BX} &= E'_0 + (P'/P)(E_D - E_0) \\ &= (E'_0 - \frac{3}{4}(P'/P)E_0) + (P'/P)(E_{2p} - E_{1s}) \\ &\approx A + (P'/P)(E_{2p} - E_{1s}), \end{aligned}$$

since  $E_{2p} = -\frac{1}{4}E_0$  and  $E_{1s} = -E_D$  ( $E_{1s}$  and  $E_{2p}$  are taken to be negative), and  $P$  is independent of the ratio of the effective masses  $\sigma = m/m_h$ , where  $m_h$  is the hole mass. Thus  $P'/P$  is the slope of the line obtained in Fig. 7.  $P'$  depends strongly on the ratio of the effective masses  $\sigma = m/m_h$ . Baldereschi<sup>19</sup> has estimated this dependence on  $\sigma$  by considering the limiting cases of a light and heavy hole, and using the appropriate hydrogen wave functions found in the literature. For an exciton bound to a neutral donor, he estimates  $P'/P \approx 0.4$  for  $\sigma = 0$  (heavy-hole case, analogous to  $H_2$  molecule), and monotonically decreasing with increasing  $\sigma$  to  $P'/P = 0.033$  as  $\sigma \rightarrow \infty$  (light-hole case, analogous to  $H^-$  ion). In applying these estimates to ZnSe and CdS, one first notes that these materials have similar values of  $\sigma$ :  $\sigma = 0.17$  for CdS,<sup>20</sup> and  $\sigma = 0.27$  for ZnSe (using our value of  $0.16m_e$  for  $m$  and  $m_h = 0.6m_e$  as determined by Aven *et al.*<sup>21</sup>). Therefore, the slopes obtained in Fig. 7 are expected to be similar. Furthermore, the slope for the  $I_2$  lines in ZnSe should be somewhat less than for CdS, as observed, since  $P'$  decreases with increasing  $\sigma$ , as discussed above. It is also expected that the slope of the line obtained for the excited states of the bound exciton complex should approach zero for the more highly excited states, since these states should not be affected by the central cell of the donor.

The donors plotted in Fig. 7 appear to show the same trends as were observed for CdS<sup>2</sup>; in that case, the lighter, more electronegative group-VII elements form deeper donors, whereas the group-III elements Ga and In appear to be inverted. For the case of ZnSe, group-III donors appear to be the principal ones, and the addition of Al confirms the trend seen in CdS. Cl is the only halogen donor which has definitely been established in ZnSe, although there is some evidence for the identification of F through the observation of its  $I_3$  doublet (cf. below). The positions of both Cl and F on this plot

are also consistent with the results in CdS, although if F has been properly identified, it is much closer to In in binding than was the case in CdS. The reasons for these trends in binding and for the different behavior of the halogen and metal-ion donors are not presently understood.

(b) *Excitons bound to ionized donors— $I_3$  lines.* For each different donor  $I_2$  line, there corresponds a doublet at somewhat lower energy (Figs. 1 and 2). The intensity ratio between the doublet and the  $I_2$  line is approximately constant for many different crystals, indicating that both are associated with the same substitutional donor. These doublets, referred to earlier in this paper as  $I_3$  lines, also yield a remarkably straight line when plotted as a function of the central-cell correction for each donor (Fig. 7). A weak fifth doublet has also been seen (apparently without a corresponding  $I_2$  line), in crystals which had been annealed in the presence of  $ZnF_2$  at  $600^\circ C$ . A tentative identification of this doublet as due to fluorine has therefore been made. When the binding energies of the components of this doublet are plotted in Fig. 7, it is found that the doublet splitting is the same as that of the other doublets, and that the corresponding  $I_2$  line could not be experimentally resolved from the indium  $I_2$  line. Unfortunately, the doublet lines are too broad for magneto-optical studies, but the straight lines plotted in Fig. 7 have slope  $m(\text{strong, weak})=0.89$ , very close to the slope of the linear relationship obtained from the  $I_3$  lines in CdS<sup>2</sup>:  $m(I_3)=0.82$ . On the basis of this evidence, the doublets are believed to be the  $I_3$  lines in ZnSe, and it is quite interesting that they are deeper than the  $I_2$  lines (i. e., excitons are more tightly bound to ionized donors than to neutral donors in ZnSe). Note, however, that the order of the  $I_3$  lines also appears to be reversed from that of CdS: The stronger member of the doublet is deeper in ZnSe, whereas the opposite is the case in CdS. It should be emphasized that symmetry assignments cannot be unambiguously made in the absence of magneto-optical studies for the states involved in these transitions, and different states may be observed for the  $I_3$  lines in cubic ZnSe than in hexagonal CdS.

Similar arguments can be made for exciton binding to ionized donors as was done above for neutral donors. In this case Baldereschi<sup>19</sup> estimates  $P'$  to be a monotonically increasing function of  $\sigma$ , with  $P'/P=0.56$  at  $\sigma=0$  ( $H_2^+$  limit) and  $P'/P=1$  as  $\sigma \rightarrow \infty$ . (The binding for this limiting case of the H atom is  $E_D$ , by definition. Actually,  $\sigma$  never reaches  $\infty$ , since the hole becomes unbound when it is too light. The critical value for binding was recently calculated by Skettrup *et al.*<sup>23</sup> to be  $\sigma_{crit}=0.426$ .) Therefore, since  $P'$  increases with  $\sigma$ , the larger slope obtained for ZnSe compared with

CdS is expected.

The fact that the  $I_3$  lines are deeper than the  $I_2$  lines in ZnSe can be understood, at least qualitatively, from the arguments of Hopfield.<sup>22</sup> The binding energy for an exciton bound to a neutral donor ( $E_{BX}$ ) is found by subtracting the free-exciton energy ( $E_{ex}$ ) from the energy for removing an electron and a hole from a neutral donor ( $E_T$ ), which was shown by Hopfield to vary from  $1.33E_D$  at  $\sigma=0$  to  $0.055E_D$  as  $\sigma \rightarrow \infty$ . On the other hand, the energy for binding an exciton to an ionized donor is approximately obtained by subtracting  $E_{ex}$  from  $E_D$  (neglecting the small energy for binding the hole to the neutral donor). Since  $E_T$  crosses  $E_D$  at a value of  $\sigma$  somewhere between 0.20 and 0.25, one expects the  $I_3$  line to be shallower than the  $I_2$  line for  $\sigma$  less than the crossover value, and deeper for larger values of  $\sigma$ . This is the effect observed in going from CdS to ZnSe. In fact, Hopfield's energy calculations predict the correct order of magnitude for this energy difference, since the energy difference between  $E_T$  and  $E_D$  is of order  $0.1E_D \approx 3$  meV for ZnSe, which is the separation between the In  $I_2$  and  $I_3$  lines.

A more quantitative estimate of the binding of an exciton to an ionized donor can be made using the results of Skettrup *et al.*,<sup>23</sup> who calculated the binding as a function of  $\sigma$  and  $E_{ex}$ . Using  $\sigma=0.27$ <sup>21</sup> and  $E_{ex} \approx 20$  meV,<sup>17</sup> one obtains 5.7-meV binding energy, which agrees well with the strong component of the Cl  $I_3$  line (cf. Fig. 7).

#### E. Donor Binding Energies

Table IV shows the donor binding energies determined from these studies by adding the effective-mass energy of the  $2p$  state to the measured value of  $E_{2p} - E_{1s}$ . The result given for F is estimated from Fig. 7 using the measured energy of the  $I_3$  lines. The donor binding energies are seen to vary from 26.3 to 29.3 meV, a spread of only 3 meV in going from the deepest to the shallowest donors observable by these doping techniques. This result is very similar to that found in CdS, and shows that non-Coulomb binding of electrons is

TABLE IV. Donor binding energies (meV).

Donor	$E_{2p} - E_{1s}$ <sup>a</sup>	$E_D$ <sup>b</sup>
Al	$19.14 \pm 0.04$	$26.3 \pm 0.6$
Cl	$19.66 \pm 0.04$	$26.9 \pm 0.6$
Ga	$20.72 \pm 0.04$	$27.9 \pm 0.6$
In	$21.69 \pm 0.04$	$28.9 \pm 0.6$
F	$22.14 \pm 0.04$ <sup>c</sup>	$29.3 \pm 0.6$

<sup>a</sup>Experimental determination.

<sup>b</sup>Using the  $2p$  effective-mass energy:  $\frac{1}{4}E_0 = 7.2 \pm 0.6$  meV.

<sup>c</sup>Extrapolated from the  $FI_3$  line using Fig. 7.

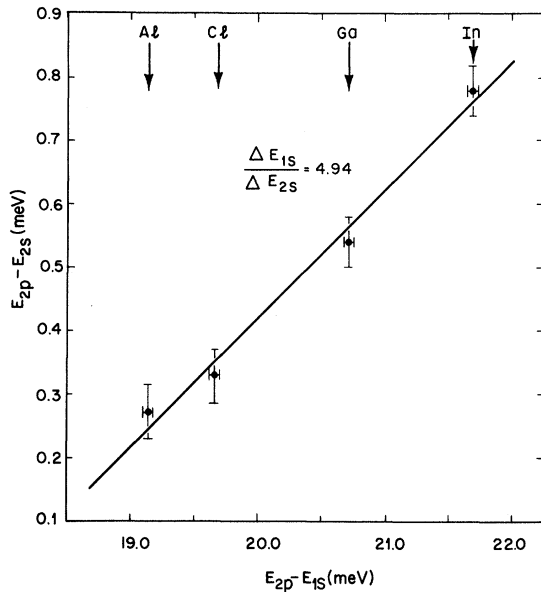


FIG. 8. Plot of  $(E_{2p}-E_{2s})$  vs  $(E_{2p}-E_{1s})$ , which shows the variation of the  $1s$  central-cell correction relative to the  $2s$  central-cell correction. The reciprocal slope of the straight line,  $\Delta E_{1s}/\Delta E_{2s}$ , is a measure of the ratio of the probability of the donor electron in the  $1s$  state to be in the central cell to that for the  $2s$  state. For a hydrogenic donor this is 8.

very small in both of these materials, as has already been pointed out for CdS.<sup>2</sup>

It is interesting to plot the energy difference  $E_{2p}-E_{2s}$  as a function of the central-cell correction  $E_{2p}-E_{1s}$  for each of the donors. This has been done in Fig. 8. The reciprocal of the slope of the straight line obtained from this plot is a measure of the ratio of the probability of the donor electron in the  $1s$  state to be in the central cell, to that for the  $2s$  state. A ratio of 8 is expected for a simply hydrogenic donor. The experimentally determined ratios are ZnSe,  $\Delta_{1s}/\Delta_{2s}=4.94$  (Fig. 8) and for CdS,  $\Delta_{1s}/\Delta_{2s}=4.46$  (Ref. 2). The discrepancy between these numbers and the expected value of 8 is not understood, but they once again demonstrate the similarity of behavior for the donors in ZnSe and CdS.

#### IV. CONCLUSIONS

By examining a large number of doped and undoped crystals grown from the vapor phase, the principal substitutional donors in cubic ZnSe have been chemically identified and their binding energies measured. The more common substitutional donors in ZnSe appear to be on cation rather than anion sites. Chemical evidence for the Ga, In, and Cl donors is quite strong; the identification of the Al donor is somewhat less definite, and it is believed that the F donor has also been observed

(by means of its  $I_3$  line). No evidence has been seen for the presence of Br or I, despite doping attempts. This is somewhat surprising, since these halogens might be expected to fit better into ZnSe than into CdS, where they have been observed.<sup>2</sup> However, in most other respects, the results found for ZnSe are closely analogous to those obtained for the other  $n$ -type II-VI compounds CdS and CdSe. Donor binding energies are found to be quite close to the effective-mass values in all three of these materials, and the small central-cell corrections observed for specific donors follow similar trends. The difference in binding energy is only 3 meV in going from the deepest to the shallowest of the observed donors.

The similarities between ZnSe and other II-VI compounds are also evident from the appearance of the  $I_2$  lines, resulting from the recombination of excitons bound to neutral donors. A series of excited states of this complex is observed. Although the magneto-optics of these  $I_2$  lines were not studied in detail, they were found to correlate closely with the donor-doping experiments, the observation of two-electron transitions, and appearance of characteristic donor-acceptor pair lines. (This last feature will be discussed in detail by MNS.)

The two-electron transition lines in the spectrum were complicated by the presence of transitions originating from the excited states of the bound exciton complex, but it was possible to distinguish the various  $2s$  and  $2p$  states by examining their behavior in a magnetic field. From these measurements the electron effective mass and the effective-mass binding energy were determined for ZnSe, as well as the actual  $E_{2p}-E_{1s}$  energy separations for each of the donors.

For each donor identified by means of its  $I_2$  lines and two-electron transitions, a doublet was observed that results from the recombination of excitons bound to the ionized donor ( $I_3$  line). These  $I_3$  lines were found to be deeper than the corresponding  $I_2$  lines, in contrast to CdS. Although the actual energy states involved in these  $I_3$ -line transitions have not been identified, theoretical estimates show that the position of the  $I_3$  lines in the ZnSe spectrum, as well as the variation of both the  $I_3$  and  $I_2$  lines as a function of donor central-cell correction, is reasonable in comparison with CdS.

#### ACKNOWLEDGMENTS

The authors would like to thank C. H. Henry for many stimulating conversations during the course of this work and A. Baldereschi for theoretical discussions of his estimates of exciton binding to neutral and ionized donors, which he has kindly made available to us prior to publication. We also

wish to thank D. T. F. Marple for discussions concerning the values of several of the constants of ZnSe, C. K. Kim for the activation analysis for Cl,

and E. A. Sadowski and A. M. Sergent for extremely competent technical assistance in all phases of the experiments.

<sup>1</sup>C. H. Henry and K. Nassau, *Phys. Rev. B* **2**, 997 (1970).

<sup>2</sup>K. Nassau, C. H. Henry, and J. W. Shiever, in *Proceedings of the Tenth International Conference of the Physics of Semiconductors*, Cambridge, Mass., 1970, edited by S. P. Keller, J. C. Hensel, and F. Stern (National Bureau of Standards, Springfield, Va., 1970), p. 629.

<sup>3</sup>C. H. Henry, K. Nassau, and J. W. Shiever, *Phys. Rev. B* **4**, 2453 (1971).

<sup>4</sup>C. H. Henry, K. Nassau, and J. W. Shiever, *Phys. Rev. B* **5**, 458 (1972).

<sup>5</sup>P. J. Dean, J. D. Cuthbert, D. G. Thomas, and R. T. Lynch, *Phys. Rev. Letters* **18**, 122 (1967).

<sup>6</sup>D. C. Reynolds, C. W. Litton, and T. C. Collins, *Phys. Rev.* **174**, 845 (1968).

<sup>7</sup>D. C. Reynolds, C. W. Litton, and T. C. Collins, *Phys. Rev.* **177**, 1161 (1969).

<sup>8</sup>D. C. Reynolds and T. C. Collins, *Phys. Rev.* **185**, 1099 (1969).

<sup>9</sup>H. Malm and R. R. Haering, *Can. J. Phys.* **49**, 2432 (1971); **49**, 2970 (1971).

<sup>10</sup>P. J. Dean and J. L. Merz, *Phys. Rev.* **178**, 1310 (1969).

<sup>11</sup>J. L. Merz, K. Nassau, and J. W. Shiever (unpublished).

<sup>12</sup>K. Nassau and J. W. Shiever, *J. Cryst. Growth* **13/14**,

375 (1972).

<sup>13</sup>Operating at discharge currents between 30 and 35 A with uv reflectors, this laser emits two lines at 3511 and 3638 Å, with an intensity ratio of ~40:60.

<sup>14</sup>A. M. Sergent (private communication).

<sup>15</sup>D. T. F. Marple, *J. Appl. Phys.* **35**, 1879 (1964).

<sup>16</sup>S. Roberts and D. T. F. Marple (unpublished). Their result is quoted in Ref. 15.

<sup>17</sup>B. Segall and D. T. F. Marple, in *Physics and Chemistry of II-VI Compounds*, edited by M. Aven and J. S. Prener (Wiley-Interscience, New York, 1967), p. 335.

<sup>18</sup>J. R. Haynes, *Phys. Rev. Letters* **4**, 361 (1960).

<sup>19</sup>A. Baldereschi, unpublished work in which the original estimates of exciton binding by J. J. Hopfield (Ref. 22) have been extended by including central-cell effects.

<sup>20</sup>J. J. Hopfield and D. G. Thomas, *Phys. Rev.* **122**, 35 (1961).

<sup>21</sup>M. Aven, D. T. F. Marple, and B. Segall, *J. Appl. Phys.* **32**, 2261 (1961).

<sup>22</sup>J. J. Hopfield, in *Proceedings of Seventh International Conference on the Physics of Semiconductors, Paris, 1964*, edited by M. Hulin (Dunod, Paris, 1964), p. 725. This work is systematically discussed by R. E. Halsted, in Ref. 17, Chap. 8, pp. 390-396.

<sup>23</sup>T. Skettrup, M. Suffczynski, and W. Gorzkowski, *Phys. Rev. B* **4**, 512 (1971).

## Microwave Photoconductivity and Luminescence of ZnS and CdS Phosphors\*†

Bernard Kramer, Samuel Gelfman,‡ and Kalman Kalikstein

*Department of Physics and Astronomy, Hunter College of the City University of New York, New York, New York 10021*

(Received 2 February 1972)

Using a microwave method for determining the true photoconductivity of ZnS and CdS powdered phosphors, and correlating these results with luminescence measurements, it is shown that the Schon-Klasens model does not hold under various conditions of excitation and additional infrared radiation. A modification of this model is proposed which takes into account the possibility that the luminescent centers have a range of differing transition probabilities. The modified model agrees with the experimental results reported here.

### I. INTRODUCTION

In a previous investigation,<sup>1</sup> a microwave method was described for measuring the photoconductivity of phosphor powders. The advantage of this method consists of the elimination of polarization effects (which are a source of error in dc and low-frequency ac measurements) and surface effects introduced by electrodes. Using this possibility of making reliable photoconductivity measurements on powders, light emission and photoconductivity were measured simultaneously in order

to facilitate the interpretation of the experimental data in terms of a suitable model.<sup>2-6</sup>

The experimental results, all at room temperature, will be described in three parts. The first will deal with the determination of the photoconductivity-light-intensity relationship and the calculation of the corresponding electron densities. The second will treat the effects obtained with simultaneous application of uv and ir radiation after equilibrium is reached. The last part will report on measurements of the rise and decay of luminescence and conductivity due to uv excita-